Macromolecules

Article

pubs.acs.org/Macromolecules

Thermally Rearrangeable PIM-Polyimides for Gas Separation Membranes

Hosna Shamsipur,[†] Bann A. Dawood,[†] Peter M. Budd,*[,†] Paola Bernardo,[‡] Gabriele Clarizia,[‡] and Johannes C. Jansen[‡]

[†]School of Chemistry, University of Manchester, Manchester M13 9PL, United Kingdom

[‡]Institute on Membrane Technology (ITM-CNR), Via P. Bucci, cubo 17/C, 87036 Rende (CS), Italy

ABSTRACT: Membrane gas separations require materials with high permeability and good selectivity. For glassy polymers, the gas transport properties depend strongly on the amount and distribution of free volume, which may be enhanced either by engineering the macromolecular backbone to frustrate packing in the solid state or by thermal conversion of a soluble precursor to a more rigid structure of appropriate topology. The first approach gives polymers of intrinsic microporosity (PIMs), while the second approach is used in thermally rearranged (TR) polymers. Recent research has sought to combine these approaches, and here a new range of thermally rearrangeable PIM-polyimides are reported, derived from dianhydrides incorporating a spiro center. Hydroxyl-functionalized polyimides were prepared using two different diamines: 2,2-bis(3-amino-4-hydroxyphenyl)hexafluoropropane (bisAPAF) and 4,6-diaminoresorcinol (DAR). Thermal treatment at 450 °C under N_2 for 1 h yielded polybenzoxazole (PBO) polymers, which showed increased permeability, compared to the precursor, in membrane gas permeation experiments. A polymer based on DAR (PIM-PBO-3) exhibited a CO_2/N_2 selectivity of 30 as prepared, higher than the values of 21−23 obtained for polymers derived from bisAPAF with the same dianhydride (PIM-PBO-1).

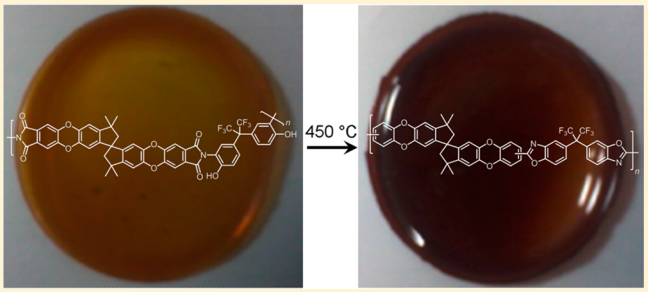

INTRODUCTION

Gas separation membranes already represent an established technology for some important industrial applications, such as the recovery of hydrogen in the production of ammonia, the separation of air to give a nitrogen-rich inert gas, and the removal of carbon dioxide from natural gas.[1,2] However, other applications, such as alkene/alkane separation and carbon dioxide capture from flue gases, require better membrane performance, in terms of productivity and product purity, if the potential of membrane processes for energy-efficient, cost-effective separations is to be fully realized. For a membrane material, productivity may be expressed in terms of a permeability coefficient, P, which in the simplest case is the product of a diffusion coefficient, D, and a solubility coefficient, S, i.e., $P = DS$. Separation efficiency or selectivity for two gases A and B may be expressed in the ideal case as a ratio of permeabilities, $\alpha_{A/B} = P_A/P_B$. For glassy polymers, which have been extensively investigated as membrane materials, the gas transport behavior is strongly influenced by the amount and distribution of free volume. In general, high free volume enhances D, and hence P, but the size and connectivity of free volume elements can strongly affect S and have a profound influence on the selectivity. In recent years various approaches have been employed in order to obtain polymers with high free volumes and desirable free volume distributions and hence to tailor the gas transport properties.[3,4]

One approach is to engineer the backbone of the polymer to give a macromolecular structure that frustrates packing in the solid state. This approach has given rise to a class of polymers termed "polymers of intrinsic microporosity" (PIMs).[5−8] These polymers have sufficient interconnected free volume for them to behave like microporous materials as defined by IUPAC[9] (pore size <2 nm).[10] Their backbone is composed of ladder (fused ring) sequences interrupted by sites of contortion, such as spiro centers, which force the backbone to twist and turn. The lack of any single bonds in the backbone about which rotation can occur means that large-scale conformational change is prohibited, although short-range flexure is possible. The archetypal PIM, referred to as PIM-1 (Figure 1a), is prepared from a spiro-containing tetrahydroxy monomer (5,5′,6,6′-tetrahydroxy-3,3,3′,3′-tetramethyl-1,1′-spirobisindane) and a tetrafluoro monomer (tetrafluoroterephthalonitrile) by a double aromatic nucleophilic substitution reaction.[8,11] Its gas separation behavior,[12,13] for important gas pairs such as O_2/N_2 and CO_2/CH_4, was shown to surpass the upper bounds of performance as given in 1991 by Robeson[14] and helped to define Robeson's revised 2008 upper bounds.[15]

Aromatic polyimides, prepared from a variety of dianhydrides and diamines, have been widely investigated as materials for gas

Received: May 29, 2014
Revised: July 18, 2014
Published: August 4, 2014

   dx.doi.org/10.1021/ma5011183 | *Macromolecules* 2014, 47, 5595−5606

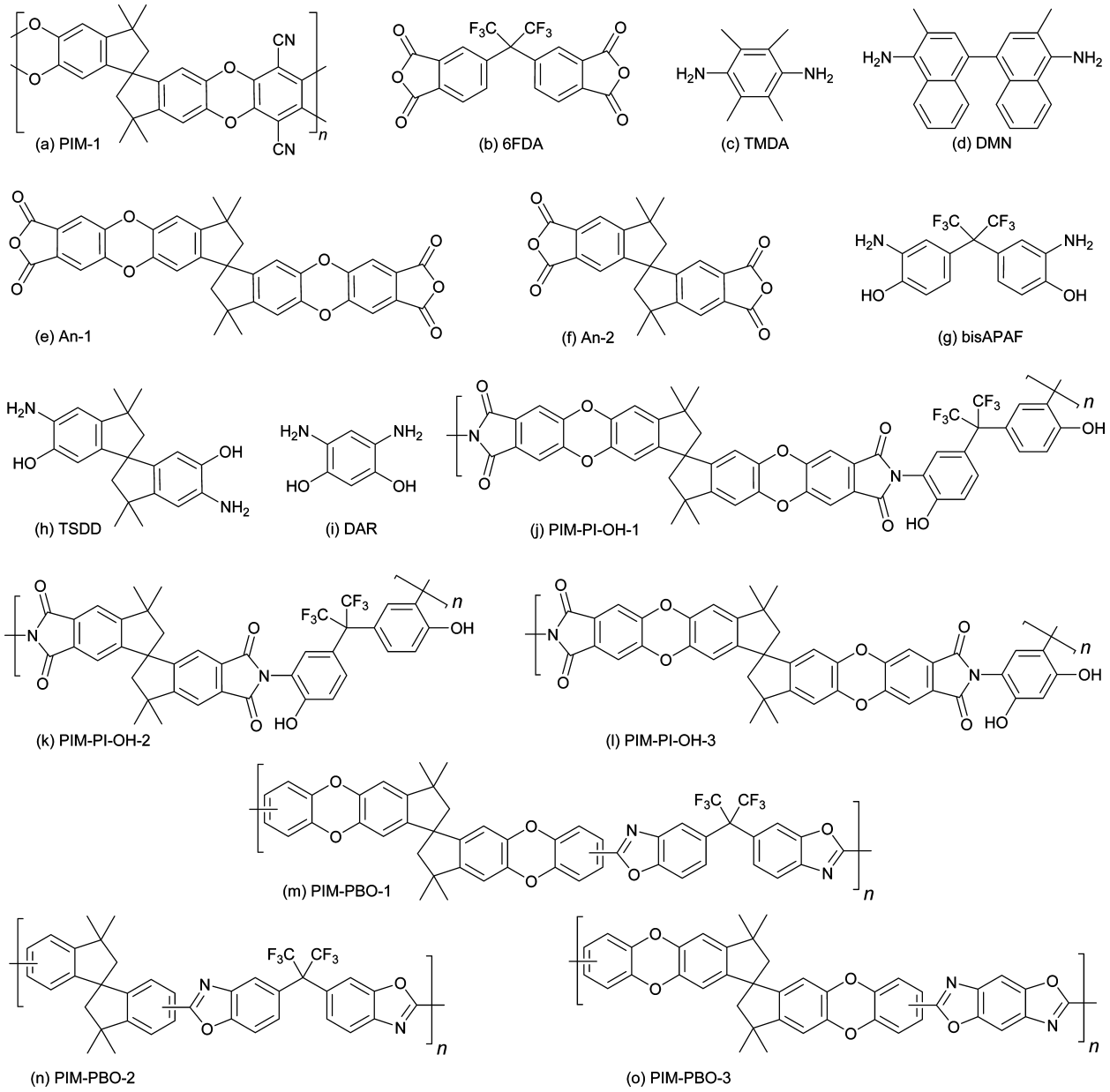

Figure 1. Chemical structures of (a) the polymer of intrinsic microporosity PIM-1, (b) 4,4′-(hexafluoroisopropylidene)diphthalic anhydride (6FDA), (c) 2,3,5,6-tetramethyl-1,4-phenylenediamine (TMDA), (d) 3,3′-dimethylnaphthidine (DMN), (e) dianhydride An-1, (f) dianhydride An-2, (g) 2,2-bis(3-amino-4-hydroxyphenyl)hexafluoropropane (bisAPAF), (h) 3,3,3′,3′-tetramethyl-1,1′-spirobisindane-5,5′-diamino-6,6′-diol (TSDD), (i) 4,6-diaminoresorcinol (DAR), and (j–o) polymers prepared in this work.

separation membranes.[16,17] A dianhydride which has attracted particular attention is 4,4′-(hexafluoroisopropylidene)diphthalic anhydride (6FDA, Figure 1b), which gives polyimides with good CO_2/CH_4 selectivity when combined with diamines such as 2,3,5,6-tetramethyl-1,4-phenylenediamine[18] (TMDA, Figure 1c) and 3,3′-dimethylnaphthidine[19] (DMN, Figure 1d).

The PIM concept has been applied in order to enhance the permeability which can be achieved with polyimides. Zhang et al.[20] and Ghanem et al.[21,22] independently established different synthetic routes to a dianhydride incorporating a spiro center (An-1, Figure 1e). The latter group investigated the gas transport properties of PIM-polyimides (PIM-PIs) prepared from An-1 with a range of diamines, showing that the permeability could be tuned by varying the structure of the diamine to give greater or less restriction to rotation about the imide linkage. In particular, exceptional permeability, coupled with selectivity at the upper bound of performance, was obtained with TMDA (giving PIM-PI-1) and DMN (giving PIM-PI-8), which have methyl groups adjacent to the amine. More recently, Rogan et al.[23] developed a spiro-containing dianhydride (An-2, Figure 1f) which does not have the relatively flexible dibenzodioxin units of An-1. PIM-polyimides PIM-PI-9 and PIM-PI-10 were prepared from An-2 with TMDA and DMN, respectively, and were shown also to exhibit high permeability compared to conventional polyimides.

A challenge for researchers seeking to develop improved polymer membranes, is that structural features desirable for high selectivity (i.e., rigid units in arrangements that give a well-defined free-volume topology) tend to give insoluble materials that cannot easily be processed. One way round this problem is

dx.doi.org/10.1021/ma5011183 | Macromolecules 2014, 47, 5595–5606

to prepare a membrane from a soluble precursor polymer and then generate the desired final structure through an irreversible molecular rearrangement. This approach was taken by Park et al.,[24] who utilized aromatic polyimides with ortho-positioned functional groups (e.g., −OH, −SH) as precursors. High-temperature treatments (350−450 °C) then gave thermally rearranged (TR) polymers, benzoxazole structures arising from hydroxyl-functionalized polyimides, and benzothiazole structures from thiol-functionalized polyimides. They showed, for example, that TR polymers derived from PIOFG-1, a polyimide prepared from 6FDA and 2,2-bis(3-amino-4-hydroxyphenyl)-hexafluoropropane (bisAPAF, Figure 1g), possessed larger free volume cavities with a narrower distribution than in the precursor and exhibited combinations of permeability and selectivity for the CO_2/CH_4 gas pair that surpassed the upper bound of performance for polymeric membranes.

Since the first report, a variety of TR polymers have been investigated,[25−33] including copolymers with pyrrolone,[34] imide,[35,36] aromatic ether,[37] and cardo[38] units. While the mechanism of thermal rearrangement has been questioned,[39−41] there is reasonable evidence for the conversion of hydroxyl-containing polyimides to benzoxazole structures.[42] Computer simulation has been used to elucidate the changes occurring on thermal rearrangement.[43,44] Sorption[45−47] and dynamic mechanical[48] studies have been undertaken. TR polymers have successfully been prepared in hollow fiber form[49] and have been employed in microfabrication.[50]

A natural progression was to seek to combine the characteristics of PIMs and TR polymers. Ma et al.[51] and Li et al.[52] independently developed synthetic routes to a hydroxyl-functionalized diamine incorporating a spiro center, 3,3,3′,3′-tetramethyl-1,1′-spirobisindane-5,5′-diamino-6,6′-diol (TSDD, Figure 1h), which was used together with 6FDA and other dianhydrides to prepare thermally rearrangeable polyimides. The latter group investigated the mechanical properties of spiro-containing TR polymers, demonstrating that incorporation of a spiro center introduces some short-range torsional freedom and gives membranes with much higher elongation at break than conventional TR polymers. Meanwhile, the first group pushed thermal treatment to the extreme, moving beyond thermal rearrangement to carbonization[53,54] and demonstrating exceptional performance for CO_2/CH_4 separation.

The present contribution concerns thermally rearrangeable PIM-polyimides derived from the spiro-containing dianhydrides An-1 (Figure 1e) and An-2 (Figure 1f). With the diamine bisAPAF (Figure 1g), An-1 and An-2 yielded the hydroxyl-containing PIM-polyimides PIM-PI-OH-1 (Figure 1j) and PIM-PI-OH-2 (Figure 1k), respectively. The synthesis of PIM-PI-OH-1 by two routes was explored: a thermal imidization method (T-PIM-PI-OH-1) and a one-pot polycondensation method (O-PIM-PI-OH-1) (Scheme 1). PIM-PI-OH-2 did not give mechanically robust membranes, so a copolymer was prepared of bisAPAF with both An-1 and An-2. A further hydroxyl-containing PIM-polyimide, PIM-PI-OH-3 (Figure 1l), was prepared from An-1 with 4,6-diaminoresorcinol (DAR, Figure 1i). Transport properties of the thermally rearranged polymers PIM-PBO-1 (Figure 1m), Copol-PBO-(1−2), and PIM−PBO-3 (Figure 1o) are discussed, and the latter in particular is shown to possess promising selectivity for the gas pair CO_2/N_2.

Scheme 1. Preparation of PIM-PI-OH by Thermal Imidization (T) and One-Pot Polycondensation (O) Methods and Thermal Rearrangement to PIM-PBO[a]

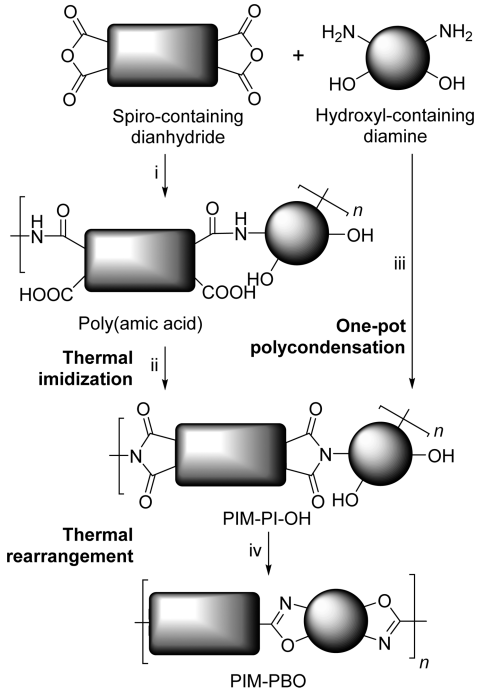

[a]Reagents and conditions: for T-PIM-PI-OH-1 (i) NMP, N_2 (ii) 300 °C, N_2; for O-PIM-PI-OH-1 (iii) *m*-cresol, quinolone, toluene, 200 °C, N_2; for PIM-PI-OH-2 (iii) NMP, quinolone, toluene, 200 °C, N_2; for PIM-PI-OH-3 (iii) NMP, 1,2-dichlorobenzene, 180 °C, N_2; for thermal rearrangement to PIM-PBO in all cases (iv) 450 °C, N_2, 1 h.

EXPERIMENTAL SECTION

Materials. Dianhydride An-1 was prepared by the method of Ghanem et al.[22] and dianhydride An-2 by the method of Rogan et al.[23] Quinoline (98%, Aldrich) was distilled under vacuum onto a 4 Å molecular sieve. Toluene (Fisher Scientific) was distilled under nitrogen from sodium metal using benzophenone as an indicator. 2-Bromopropene (Aldrich) was distilled freshly prior to use. *m*-Cresol (Lancaster) and *N*-methyl-2-pyrrolidone (NMP, Sigma-Aldrich, 97%) were distilled prior to use. Anhydrous 1,2-dichlorobenzene (Sigma-Aldrich, 99%) was stored over molecular sieve. 1,4,5,8-Naphthalene-tetracarboxylic dianhydride (97%, Aldrich), 2,2-bis(3-amino-4-hydroxyphenyl)hexafluoropropane (bisAPAF, 98%, TCI), 4,6-diaminoresorcinol dihydrochloride (DAR·2HCl, Sigma-Aldrich, 97%), tetrahydrofuran (THF, Aldrich), anhydrous *o*-xylene (Aldrich), $KMnO_4$ (Aldrich), and pyridine (Aldrich) were used as received.

Preparation of PIM-PI-OH-1 by Thermal Imidization Method. An-1 (0.500 g, 0.796 mmol), bisAPAF (0.290 g, 0.796 mmol), and freshly distilled NMP (25 mL) were added to a 50 mL two-neck round-bottom flask and heated to 80 °C to dissolve and then left to stir overnight under N_2. To obtain a membrane, the poly(amic acid) (PAA) solution was cast into a Petri dish, solvent removed using a vacuum oven at 80 °C for 1 h, and then heated in an oven for 1 h at 300 °C to achieve conversion to PIM-PI-OH-1. For batch HS77: IR (ATR; cm^{-1}): 3400 (OH stretching), 1780 (symmetric C=O stretching), 1710 (asymmetric C=O stretching), 1360 (C−N stretching). Anal. Calcd for $C_{52}O_{10}N_2F_6H_{32}$: C, 65.14; H, 3.36; N, 2.92. Found: C, 63.60; H, 2.73; N, 3.37. MALDI-TOF MS: *m*/*z* 1941, 2899, 3857, 4815. BET surface area = 360 $m^2\ g^{-1}$.

Preparation of PIM-PI-OH-1 by One-Pot Polycondensation Method. An-1 (0.500 g, 0.796 mmol), bisAPAF (0.290 g, 0.796 mmol), distilled and dried *m*-cresol (5 mL), quinolone (0.1 mL), and toluene (2 mL) were added to a 50 mL two-neck round-bottom flask equipped with a Dean−Stark trap and a condenser. The toluene helps

dx.doi.org/10.1021/ma5011183 | Macromolecules 2014, 47, 5595−5606

to remove water azeotropically. The mixture was stirred under N_2, and the heater temperature gradually increased to 200 °C over 1 h, during which time toluene evaporates with produced water and collects in the Dean−Stark trap, and then kept at that temperature for 5 h. After cooling, the mixture was diluted with THF (5 mL) and the product recovered by precipitation in toluene. The precipitate was filtered off and dried in a vacuum oven at 180 °C for at least 5 h. For batch HS110: ^{1}H NMR (pyridine-d_5; 400 MHz) δ (ppm): 1.31 (6H, br s, CH_3), 1.38 (6H, br s, CH_3), 2.19 (2H, d, J = 9.58 Hz, CH_2), 2.31 (d, 2H, J = 11.10 Hz, CH_2), 6.49 (2H, br s, Ar), 6.79 (2H, s, Ar), 7.22 (2H, br s, Ar), 7.24 (2H, br s, Ar), 7.52 (2H, s, Ar), 7.57 (2H, s, Ar), 8.01 (2H, br s, Ar), 13.26 (2H, br s, OH). IR (ATR; cm^{-1}): 3400 (OH stretching), 1780 (symmetric C═O stretching), 1710 (asymmetric C═O stretching), 1360 (C−N stretching). Anal. Calcd for $C_{52}O_{10}N_2F_6H_{32}$: C, 65.14; H, 3.36; N, 2.92. Found: C, 63.24; H, 4.22; N, 3.36. MALDI-TOF MS: m/z 2897, 3855, 4813, 5771.

Preparation of PIM-PI-OH-2. Dianhydride An-2 (1.500 g, 3.604 mmol), bisAPAF (1.320 g, 3.604 mmol), distilled and dried NMP (15 mL), quinolone (0.1 mL), and toluene (2 mL) were added to a 50 mL two-neck round-bottom flask equipped with a Dean−Stark trap, nitrogen inlet, and condenser. The mixture was stirred under N_2, and the temperature gradually increased to 200 °C over 1 h and then kept at that temperature for 5 h. The resulting orange-colored mixture was allowed to cool and then added dropwise to vigorously stirred methanol. The cream-colored precipitate was collected by filtration and dried in a vacuum oven at 180 °C for 5 h (90% yield). ^{1}H NMR (pyridine-d_5; 400 MHz) δ (ppm): 1.39 (6H, br s, CH_3), 1.45 (6H, br s, CH_3), 2.31 (2H, br s, CH_2), 2.48 (2H, d, J = 10.8 Hz, CH_2), 7.27−8.58 (10H, m, Ar), 13.24 (2H, br s, OH). IR (ATR; cm^{-1}): 3300 (OH stretching), 1776 (symmetric C═O stretching), 1706 (asymmetric C═O stretching), 1371 (C−N stretching). Anal. Calcd for $C_{40}O_6N_2F_6H_{28}$: C, 64.35; H, 3.78; N, 3.75. Found: C, 61.48; H, 3.61; N, 3.48. MALDI-TOF MS: m/z 2262, 3007, 3752, 4497, 5244. GPC (DMAc): M_n = 14 000; M_w = 66 000 g mol^{-1}; M_w/M_n = 4.7.

Preparation of Copol-OH-(1−2). An-1 (0.7547 g, 1.201 mmol), An-2 (0.500 g, 1.201 mmol), bisAPAF (0.8797 g, 2.402 mmol), m-cresol (10 mL), quinolone (0.1 mL), and toluene (2 mL) were added to a 50 mL two-neck round-bottom flask equipped with a Dean−Stark trap, nitrogen inlet, and condenser. The mixture was stirred under N_2, and the temperature gradually increased to 200 °C over 1 h and then kept at that temperature for 5 h. The resulting mixture was allowed to cool and then added dropwise to vigorously stirred water. The precipitate was collected by filtration and dried in a vacuum oven at 180 °C for 24 h (82% yield). ^{1}H NMR (DMSO-d_6; 400 MHz) δ (ppm): 1−2 (12H, br m, CH_3), 2−3 (4H, br m, CH_2), 6−8 (12H, br, Ar), 10.4 (1H, s, OH), 10.5 (1H, s, OH). IR (ATR; cm^{-1}): 3300 (OH stretching), 1780 (symmetric C═O stretching), 1706 (asymmetric C═O stretching), 1373 (C−N stretching). GPC (THF): M_n = 31 000; M_w = 138 000 g mol^{-1}; M_w/M_n = 4.5.

Preparation of PIM-PI-OH-3. PIM-PI-OH-3 was prepared by a modified procedure of Moy et al.[55] Because of the extreme instability of DAR, it was purchased as the dihydrochloride, and no hydrogen acceptor was used in the polymerization. DAR·2HCl was not soluble in organic solvents, but dissociated to HCl and the diamine on heating. An-1 (0.500 g, 0.796 mmol), DAR·2HCl (0.169 g, 0.796 mmol), distilled NMP (5 mL), and dried 1,2-dichlorobenzene (1 mL) were added to a 50 mL two-neck round-bottom flask equipped with a Dean−Stark trap, nitrogen inlet, and condenser. The mixture was stirred under N_2, and the temperature gradually increased to 180 °C over 1 h and then kept at that temperature overnight. After cooling, the mixture was diluted with NMP (2 mL), and the product was recovered by precipitation in vigorously stirred methanol. The brownish precipitate was collected by filtration and dried in a vacuum oven at 150 °C for 5 h (95% yield). For batch HS130: ^{1}H NMR (pyridine-d_5; 400 MHz) δ (ppm): 1.35 (6H, br s, CH_3), 1.41 (6H, br s, CH_3), 2.21 (2H, m, CH_2), 2.35 (2H,m,CH_2), 6.55 (2H, s, Ar), 6.85 (2H, s, Ar), 6.89 (1H, s, Ar), 7.55 (2H, s, Ar), 7.6 (2H,s, Ar), 7.86 (1H, s, Ar), 12.6 (2H, br s, OH). IR (ATR; cm^{-1}): 3200−3500 (OH stretching), 1778 (symmetric C═O stretching), 1720 (asymmetric C═O stretching), 1356 (C−N stretching). Anal. Calcd for $C_{43}O_{10}N_2H_{28}$: C, 70.49; H, 3.85; N, 3.82. Found: C, 68.40; H, 3.73; N, 4.02. MALDI-TOF MS: m/z 1488, 2221, 2953, 3685. GPC (DMA, 0.05% $LiNO_3$): M_n = 4700; M_w = 13 500 g mol^{-1}; M_w/M_n = 2.9. BET surface area = 430 m^2 g^{-1}.

Membrane Formation. Dense films were cast by solvent evaporation. T-PIM-PI-OH-1, prepared by the thermal imidization method, was cast to form a membrane at the poly(amic acid) stage, as described above. O-PIM-PI-OH-1 (0.0910 g), prepared by the one-pot polycondensation method, was dissolved in THF (5 mL), filtered, and cast into a leveled, flat-bottomed, 4.8 cm Petri dish, with a lid to control solvent evaporation. PIM-PI-OH-2 was not soluble in low boiling solvents such as THF and $CHCl_3$; attempts were made to cast membranes from NMP and DMA at 50 °C, but the resulting films were highly brittle and could not be used for permeation studies. Copol-OH-(1−2) and PIM-PI-OH-3 were cast from THF, as for PIM-PI-OH-1. PIM-PI-OH-3 was only partially soluble in THF, so insoluble material was filtered out prior to casting. Membranes of PIM-PI-OH-3 were also cast from DMA on a hot plate at 50 °C.

Thermal Rearrangement. Heat treatment of both powder and membrane samples was carried out in a Carbolite (Hope, UK) three zone tube furnace (11 cm i.d.) under a steady flow of N_2. Samples were treated at 450 °C for 1 h.

Characterization Methods. Elemental analyses were carried out using a Thermo Scientific Flash 2000 organic elemental analyzer (CHNS analyzer).

Attenuated total reflectance (ATR) infrared (IR) spectroscopy was undertaken on membrane samples using an ATI Mattson Genesis FTIR spectrometer.

Matrix-assisted laser desorption/ionization (MALDI) mass spectrometry was carried out using a Shimadzu Axima Confidence instrument, with dithranol as the matrix. Samples were prepared as follows. An aqueous solution of NaI (10 mg mL^{-1}) was prepared and added to the plate. A solution of the polymer in THF (10 mg mL^{-1}) was prepared and mixed (ratio 1:10) with a solution of the matrix (10 mg mL^{-1}), and the mixture was added to the NaI on the plate.

^{1}H NMR spectra were recorded on a Bruker 400 MHz spectrometer. Samples were prepared by dissolving about 5 mg of polymer in the solvent and filtering through glass wool.

High-powered decoupling (Hpdec) magic-angle spinning (MAS) solid-state ^{13}C NMR spectra were collected using a Bruker Avance III 400 MHz instrument, using adamantane as reference. Powder samples were packed into a 4 mm zirconia rotor, and a spinning rate of ca. 10 000 Hz was used. Spectra were compiled from 6000 scans using a repetition time of 10 s and a spectral width of 600 ppm.

Gel permeation chromatography (GPC) was carried out using either tetrahydrofuran (THF) or dimethylacetamide (DMAc) as mobile phase at a flow rate of 1 cm^3 min^{-1}, a sample concentration of 1 mg mL^{-1}, and an injection volume of 0.1 mL, using a Viscotek GPC max VE2001 solvent/sample module with two mixed-B and a 500 Å Polymer Laboratories PLgel columns, calibrated with polystyrene standards.

N_2 adsorption/desorption measurements of powder samples were performed on a Micromeritics ASAP 2010 instrument. A small amount of powdered sample (ca. 0.1 g) was weighed into an analysis tube which was subjected to an automatic overnight degas at a pressure of ca. 50 μmHg at a temperature of 120 °C. After reweighing the degassed sample, the N_2 adsorption/desorption analysis was undertaken at a temperature of 77 K. The apparent surface area was calculated from the adsorption data by the multipoint Brunauer−Emmet−Teller (BET) analysis.

Thermogravimetric analysis (TGA) was carried out on the PIM-PI-OH polymers using a Seiko Instruments SSC/5200 instrument with a heating rate of 5 °C min^{-1}. The purge gas was N_2 with a flow rate of 10 cm^3 min^{-1}.

Tensile tests on the membranes were carried out at room temperature on a Zwick/Roell single column Universal Testing Machine, model Z2.5, equipped with a 50 N load cell and flat ground steel pneumatic clamps. Specimens with an effective length of 20 or 30 mm (distance between the clamps) and a width of 5 mm were tested at a deformation rate of 2 or 3 mm min^{-1} (= 10% min^{-1}).

dx.doi.org/10.1021/ma5011183 | Macromolecules 2014, 47, 5595−5606

Membrane Permeation Measurements. Single gas permeation measurements were carried out in a fixed volume/pressure increase apparatus (GKSS, Germany) at 25 °C at a feed pressure of 1 bar. The instrument is equipped with PC controlled pneumatic valves to allow response times of less than 0.5 s.[56] An alumina trap on the rotary vacuum pump avoids oil contamination of the membrane. Circular samples with an effective membrane area of 2.14 cm^2 inside the footprint of the sealing ring were used. The thickness of the films was measured with a digital micrometer (Mitutoyo, model IP65). The gases were tested in the following order: He, H_2, N_2, O_2, CH_4, and CO_2. Before each experiment, the membrane sample was carefully evacuated (10^{-2} mbar) to remove previously dissolved gas species. The films were first tested "as prepared" and then after soaking overnight in ethanol and subsequent drying in air at room temperature. The data were elaborated by applying the time lag method,[57] obtaining the permeability coefficient, P, and diffusion coefficient, D, as described previously,[56] from the pressure increase curve:

$$p_t = p_0 + (\mathrm{d}p/\mathrm{d}t)_0 t + \frac{RTAl}{V_P V_m} p_f S\left(\frac{Dt}{l^2} - \frac{1}{6} - \frac{2}{\pi^2}\sum_1^\infty \frac{(-1)^n}{n^2}\exp\left(-\frac{Dn^2\pi^2 t}{l^2}\right)\right) \quad (1)$$

reducing in the steady state to

$$p_t = p_0 + (\mathrm{d}p/\mathrm{d}t)_0 t + \frac{RTA}{V_P V_m}\frac{p_f P}{l}\left(t - \frac{l^2}{6D}\right) \quad (2)$$

in which p_t is the permeate pressure at time t. p_0 and $(\mathrm{d}p/\mathrm{d}t)_0$ are the starting pressure and the baseline slope, respectively, which are normally negligible if the membrane is defect-free and sufficiently degassed. R is the universal gas constant, T the absolute temperature, A the exposed membrane area, V_P the permeate volume, V_m the molar volume of a gas at standard temperature and pressure (0 °C and 1 atm), p_f the feed pressure, S the solubility, D the diffusion coefficient, and l the membrane thickness. D is obtained from the so-called time lag, Θ, in the last term of eq 2:

$$\Theta = \frac{l^2}{6D} \quad (3)$$

The solubility coefficient for the gas in the polymer matrix was evaluated indirectly from $S = P/D$, assuming the validity of the solution-diffusion permeation model.[58] The ideal selectivity for a pair of gases, A and B, was calculated as the ratio of the individual single gas permeabilities and can be decoupled into solubility−selectivity and diffusivity−selectivity:

$$\alpha_{A/B} = \frac{P_A}{P_B} = \frac{S_A}{S_B}\frac{D_A}{D_B} \quad (4)$$

RESULTS AND DISCUSSION

PIM-PI-OH-1. Two methods were explored for preparing the hydroxyl-containing polyimide PIM-PI-OH-1 from An-1 and bisAPAF (Scheme 1). The thermal imidization (T) method involves the production of a poly(amic acid) intermediate, from which the polyimide is subsequently formed by cyclodehydration at 300 °C. In the one-step polycondensation (O) method, polymerization and imidization take place in homogeneous solution with an azeotroping agent. Both routes yielded the expected product, as demonstrated by ^{1}H NMR and IR spectroscopy and MALDI mass spectrometry (see Experimental Section). The peaks observed by MALDI, which is only able to resolve low molar mass oligomers, up to a molar mass of 5771 g mol^{-1}, correspond to cyclic structures of 3−6 repeat units with associated Na^+. The linear polymers with much higher molar mass were not detected by MALDI.

Table 1. Polystyrene-Equivalent Weight-Average Molar Mass (M_w, g mol^{-1}), Number-Average Molar Mass (M_n, g mol^{-1}), and Polydispersity (M_w/M_n) from GPC for Representative Batches of Polymers

polymer	batch	M_w	M_n	M_w/M_n
T-PIM-PAA-1[a]	HS72	64 000	31 000	2.1
	HS82	43 000	16 000	2.7
	HS148	25 000	13 000	1.9
O-PIM−PI-OH-1[a]	HS61	110 000	45 000	2.4
	HS84	1 145 000	450 000	2.5
	HS110	123 000	40 000	3.1
PIM-PI-OH-2[b]	HS98	66 000	14 000	4.7
Copol-OH-(1−2)[a]	HS161	138 000	31 000	4.5
PIM-PI-OH-3[b]	HS130	13 500	4 730	2.9
	HS133	7 320	3 170	2.3

[a]Analyzed in THF. [b]Analyzed in DMAc.

Average molar masses from GPC are given in Table 1 for various batches of poly(amic acid) from the T method (the thermally generated polyimide was only partially soluble in common organic solvents, presumably because some thermal cross-linking occurred) and polyimide from the O method. The O method gave significantly higher molar masses than the T method, but both methods gave polymers capable of forming self-supported membranes. Polyimides produced by both routes had significant internal surface area, as demonstrated by nitrogen adsorption on powder samples at 77 K, although the kinetics of adsorption was slow, leading to distorted isotherms at low pressure. While the values should be treated with caution, BET surface areas were obtained of 360 m^2 g^{-1} for T-PIM-PI−OH-1 batch HS82 and 230 m^2 g^{-1} for O-PIM-PI-OH-1 batch HS61. These values are lower than those commonly reported in the literature for PIM-1 (720−820 m^2 g^{-1}) and for PIM-PIs based on the dianhydride An-2.[23] A substantially lower value (200 m^2 g^{-1}) was, however, determined for a PIM-PI containing a spiro center both in the dianhydride An-2 and in the diamine (PIM-PI-11).[23] The reduced apparent surface area for O-PIM-PI-OH-1, compared to the T polymer which had been imidized at 300 °C, may be attributed to the presence of residual high boiling solvents that are not easily removed by the outgas conditions. For example, the IR spectrum of O-PIM-PI-OH-1 batch HS84 showed a peak at 1664 cm^{-1}, which can be assigned to the C═N of quinoline, which disappeared only after heating to 300 °C.

PIM-PI-OH-2. PIM-PI-OH-2 was prepared from the smaller dianhydride An-2 and bis-APAF using the O method, which was found to yield higher molar masses than the T method. The structure was confirmed by ^{1}H NMR, IR, and MALDI (see Experimental Section). The product proved insoluble in low boiling point solvents such as THF and $CHCl_3$, so GPC was performed in dimethylacetamide (DMAc). Although the molar mass (Table 1) was reasonably high, attempts to cast membranes from solvents such as DMAc and *N*-methyl-2-pyrrolidone (NMP) at 50 °C led to brittle, cracked films. This could be ascribed to the more rigid structure of An-2 with respect to the An-1 containing the relatively flexible dibenzodioxin units.[23] High backbone stiffness alone does not, in principle, preclude the formation of mechanically resistant films,[59] so an additional factor may be the relatively poor solubility of the polymer, unable to give a nicely entangled

dx.doi.org/10.1021/ma5011183 | Macromolecules 2014, 47, 5595−5606

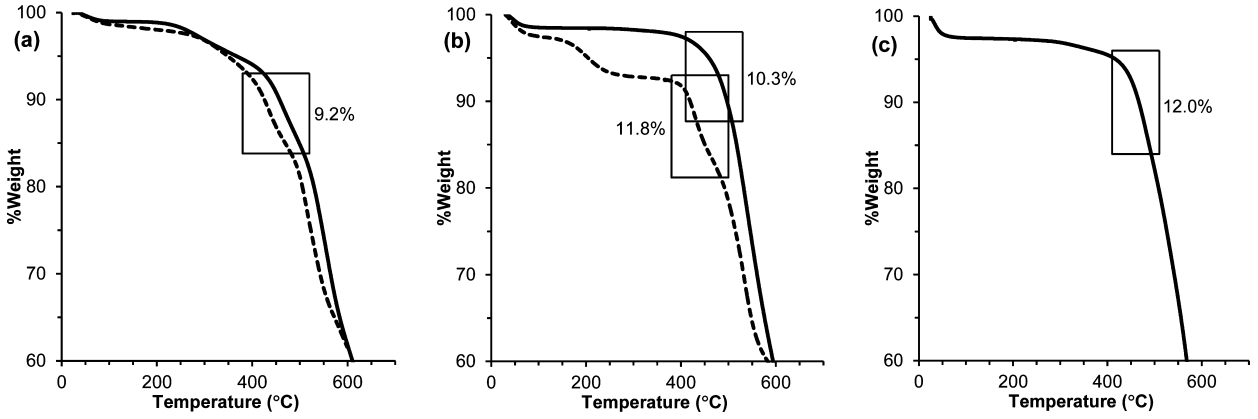

Figure 2. Thermogravimetric analysis of powder samples of (a) T-PIM-PI-OH-1 (- - -) and O-PIM-PI-OH-1 (—), (b) PIM-PI-OH-2 (- - -) and Copol-OH-(1−2) (—), and (c) PIM-PI-OH-3. The rectangular boxes indicate the theoretical weight changes upon loss of CO_2 during the TR reaction.

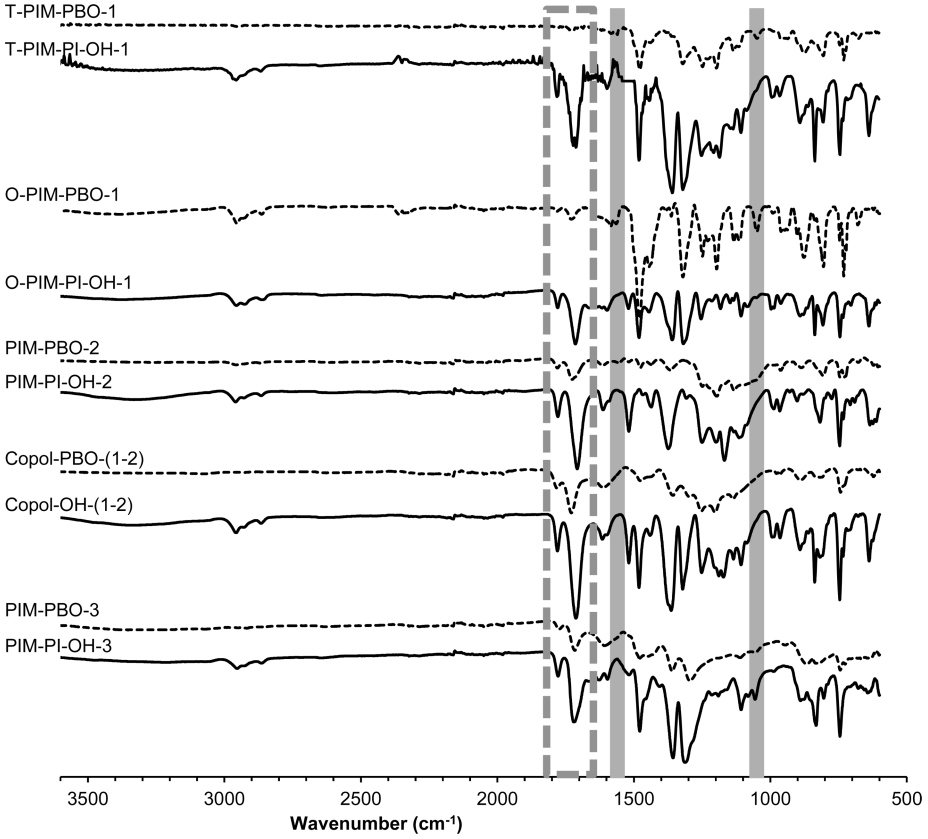

Figure 3. ATR-IR spectra of hydroxyl-containing polyimides (—) and thermally rearranged polymers (- - -). The dashed gray box indicates the position of imide carbonyl peaks, and the thick gray lines indicate approximate positions of peaks which can be attributed to benzoxazole C═N.

polymer film upon drying of the solution. The polydispersity as expressed by the ratio M_w/M_n in Table 1 was significantly higher than the value of 2.0 expected for an ideal linear step-growth polymerization; this may be attributed to branching and/or cyclic formation.

Copol-OH-(1−2). To obtain a polymer with better solubility for membrane casting, a copolymer was prepared of bisAPAF with a mixture of An-1 and An-2 (mole ratio of reactants bisAPAF:An-1:An-2 = 2:1:1). The structure was confirmed by ^{1}H NMR and IR (see Experimental Section). ^{1}H NMR showed two peaks, at 10.4 and 10.5 ppm in DMSO-d_6, for phenolic protons, indicating slightly different environments attributable to An-1 and An-2. GPC (Table 1) indicated that a high molar mass polymer was achieved. Dense and self-standing membranes of the copolymer were cast from THF.

PIM-PI-OH-3. To obtain a polymer with a higher concentration of thermally rearrangeable groups, PIM-PI-OH-3 was prepared from An-1 with the compact diamine DAR. The structure was confirmed by ^{1}H NMR, IR, and MALDI (see Experimental Section). Nitrogen adsorption of a powder sample at 77 K gave a BET surface area of 430 m^2 g^{-1}, higher than for PIM-PI-OH-1. Only modest molar masses were achieved (Table 1), but the products were nevertheless film-forming. PIM-PI-OH-3 was soluble in DMAc, NMP, and

dx.doi.org/10.1021/ma5011183 | Macromolecules 2014, 47, 5595−5606

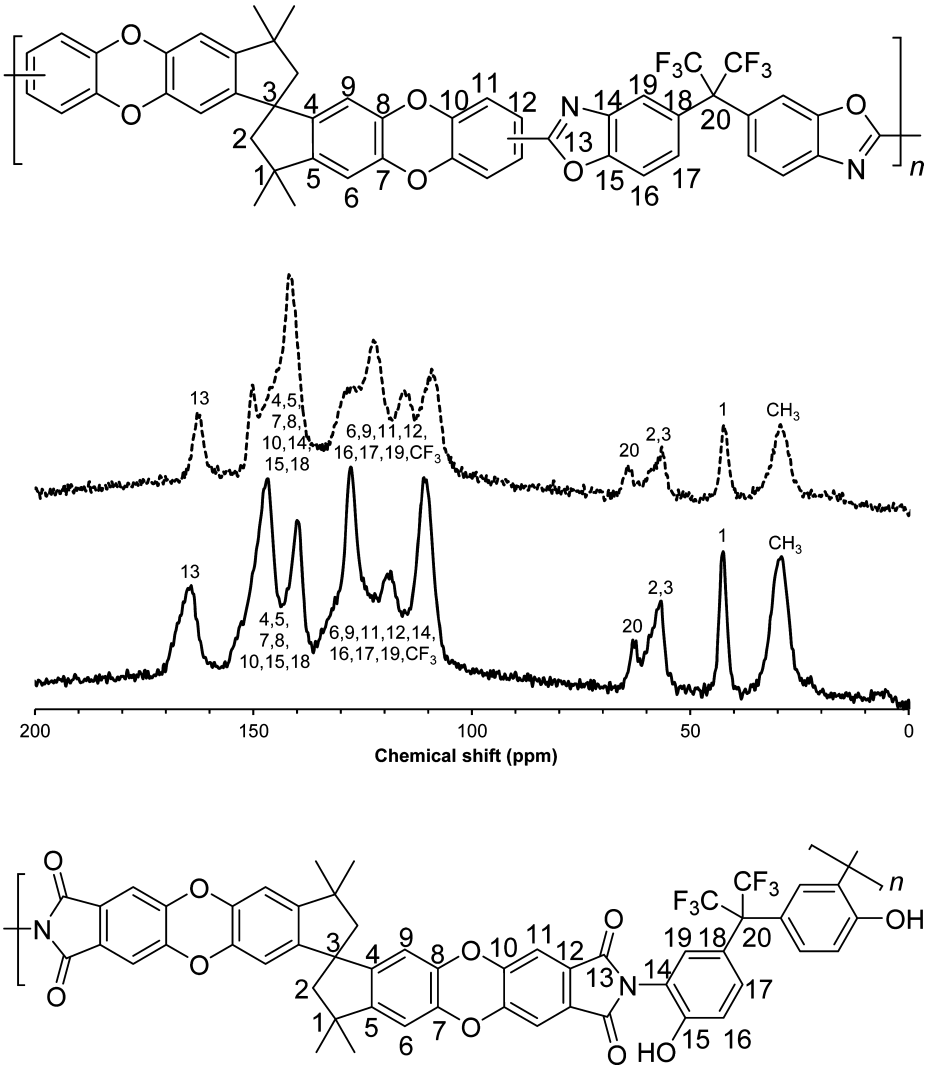

Figure 4. Solid state ^{13}C NMR spectra of T-PIM-PI-OH-1 (bottom) and T-PIM-PBO-1 (top), showing peak assignments.

Table 2. Mechanical Properties Determined by Tensile Tests for Representative Membranes

polymer	batch	no. tests	Young's modulus (MPa)	tensile strength (MPa)	elongation (%)
T-PIM-PI-OH-1	HS148	1	1080	12	1.2
T-PIM-PBO-1		4	1230 ± 120	51 ± 11	6.6 ± 3.2
Copol-PBO-(1−2)	HS161	2	680 ± 68	7.37 ± 0.34	1.29 ± 0.38
PIM−PBO-3	HS130	1	1360	12.9	1.1

pyridine and partially soluble in THF. Membranes for permeation studies were cast from THF, after filtering out insoluble material.

Thermal Rearrangement. While a rearrangement reaction is strictly a transformation between structural isomers, the term "thermal rearrangement" has previously been used in the membrane literature for the conversion of a hydroxyl-containing polyimide to a polybenzoxazole with loss of CO_2, and that terminology is retained here. TGA curves of representative powder samples of the polymers are shown in Figure 2. Marked on the plots are the weight changes expected from loss of CO_2 on thermal conversion to the ideal polybenzoxazole (PBO) structure. The small weight loss below 100 °C is probably related to the release of light gases and water vapor absorbed upon contact with the air. Weight losses in the temperature range 100−400 °C can be attributed to residual solvent. Quinoline and *m*-cresol, used in polymerization by the O method, are trapped by the polymer and are only eliminated above 200 °C. Thermal rearrangement is expected to occur at temperatures in the range 400−500 °C, with higher temperatures leading to polymer degradation and, eventually, carbonization. Other reactions may also occur at lower temperatures over longer time scales than in a TGA experiment. In the present work, polymers were thermally treated at 450 °C for 1 h under N_2. Membrane samples of T-PIM-PI-OH-1 batch HS77 and O-PIM-PI-OH-1 batch HS84, when subjected to these conditions, gave weight losses of 21% and 22%, respectively, greater than expected for thermal rearrangement alone, indicating that some additional degradation reactions also occurred.

Chemical changes on thermal treatment were monitored by IR (Figure 3). Carbonyl peaks at ca. 1710 and 1780 cm^{-1}

dx.doi.org/10.1021/ma5011183 | *Macromolecules* 2014, 47, 5595−5606

Table 3. Gas Permeability Coefficients (P) and Ideal Selectivity ($\alpha_{ij} = P_i/P_j$) for Various Gas Pairs in Representative Hydroxyl-Containing Polyimide and Thermally Rearranged Polymer Membranes at 25 °C

			P (barrer)						P_i/P_j				
polymer	batch	history	He	H_2	O_2	N_2	CO_2	CH_4	He/N_2	H_2/CH_4	O_2/N_2	CO_2/N_2	CO_2/CH_4
T-PIM-PI-OH-1	HS148	as cast	99	114	17	3.1	81	2.3	32	50	5.4	26	35
T-PIM-PBO-1	HS148	as prepared	244	360	70	16	348	16	15	23	4.3	21	22
		ethanol-treated	434	755	187	52	948	56	7.5	13	3.6	18	17
O-PIM-PI-OH-1	HS84	as cast	33	35	4.3	0.84	24	0.69	40	51	5.1	28	35
O-PIM-PBO-1	HS84	as prepared	160	245	47	11	257	10	15	25	4.3	23	26
		ethanol-treated	479	881	226	64	1176	69	7.5	13	3.5	18	17
		aged 270 days	347	555	111	26	564	26	13	21	4.3	22	22
Copol-PBO-(1−2)	HS161	as prepared	236	332	59	13	300	10	18	32	4.4	22	29
		ethanol-treated	516	895	218	58	1140	62	9.0	15	3.8	20	19
PIM-PBO-3	HS130	as prepared	184	290	42	8.3	248	9.4	22	31	5.1	30	26
		ethanol-treated	400	768	134	35	870	40	11	19	3.8	25	22
		aged 197 days	177	277	39	7.2	235	7.4	25	38	5.5	33	32

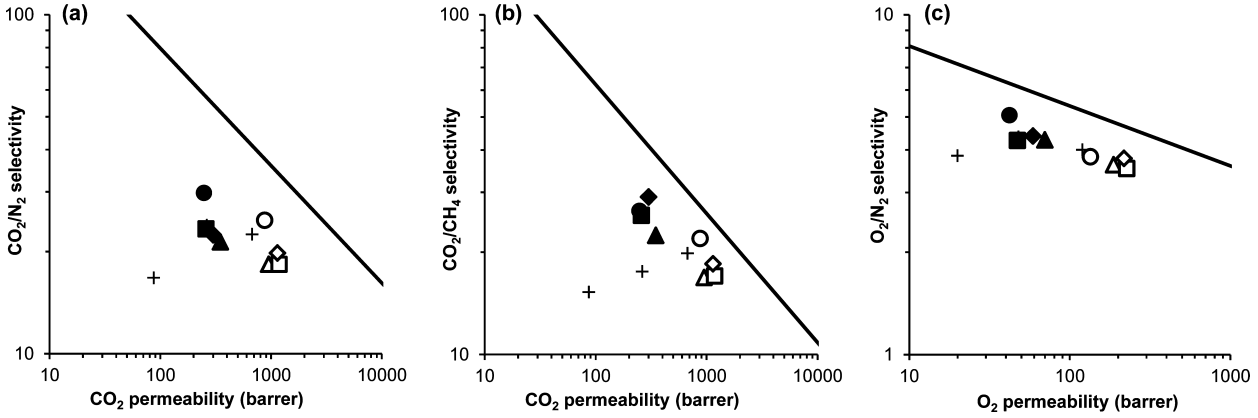

Figure 5. Double-logarithmic "Robeson" plots of (a) CO_2/N_2, (b) CO_2/CH_4, and (c) O_2/N_2 selectivity versus the permeability of the fastest gas, showing Robeson's 2008 upper bound (−),[15] with data for as prepared (solid symbols) and ethanol-treated (open symbols) PIM-PBO membranes. Data of T-PIM-PBO-1 batch HS148 (▲, △), O-PIM-PBO-1 batch HS84 (■, □), Copol-PBO-(1−2) (◆, ◇), and PIM-PBO-3 (●, ○), compared with literature data for thermally treated, spiro-containing polymers from Li et al. (+).[52]

diminished, while peaks developed at ca. 1050 and 1560 cm^{-1} that can be attributed to benzoxazole C═N.[34] In most cases, traces of imide peaks remained after thermal treatment, indicating that the extent of thermal rearrangement did not in practice reach 100%. The conversion of T-PIM-PI-OH-1 to T-PIM-PBO-1 was also investigated by solid-state ^{13}C NMR (Figure 4), which showed changes consistent with benzoxazole formation.

Thermal treatment of PIM-PI-OH-1 powder increased the BET surface area, from 360 to 440 $m^2\ g^{-1}$ for T-PIM-PBO-1 and from 230 to 405 $m^2\ g^{-1}$ for O-PIM-PBO-1, indicating an increase in microporosity. In contrast, thermal treatment of PIM-PI-OH-3 led to a slight reduction in BET surface area, from 430 $m^2\ g^{-1}$ for PIM-PI-OH-3 to 360 $m^2\ g^{-1}$ for PIM-PBO-3, suggesting some collapse of the pre-existing structure. In general, solubility in common organic solvents was lost on thermal treatment, although T- and O-PIM-PBO-1 were partially soluble in NMP on heating.

Mechanical Properties. Both the original and the thermally rearranged samples proved stiff and very brittle, making it difficult to cut enough sample specimens for tensile tests reliably. Typical results (Table 2) show that the Young's modulus often exceeds 1 GPa and that the samples break just above 1% deformation, except for sample T-PIM-PBO-1 (batch HS 148), which was relatively tough ($\varepsilon = 6.6 \pm 3.2\%$). Further optimization of these materials is necessary to enhance their mechanical properties.

Gas Permeation. Gas permeability coefficients of representative membranes with different histories, and ideal selectivities for various gas pairs, are given in Table 3. The membranes were tested "as prepared" and also after a soaking in ethanol. An alcohol treatment (soaking in methanol or ethanol overnight and then allowing to dry) is often used to eliminate effects of membrane aging as well as to remove residual solvents arising from membrane preparation.

For "as prepared" membranes, the hydroxyl-containing polyimide PIM-PI-OH-1 prepared by the thermal imidization (T) method gave similar selectivities, but higher permeabilities, than the polymer prepared by the one-pot polycondensation (O) method. The lower permeability of O-PIM-PI-OH-1 is consistent with the lower BET surface area determined by N_2 adsorption on powder samples.

For both T-PIM-PI-OH-1 and O-PIM-PI-OH-1, thermal conversion to the corresponding PBOs led to increases in permeability, with corresponding reductions in selectivity. The thermally treated copolymer, Copol-PBO-(1−2), showed similar permeabilities, with similar or higher selectivities, compared to T- and O-PIM-PBO-1. For PIM-PBO-3, permeabilities were in the same range as the PIM-PBO-1 samples, but He/N_2 and CO_2/N_2 selectivities were enhanced.

dx.doi.org/10.1021/ma5011183 | Macromolecules 2014, 47, 5595−5606

Table 4. Gas Diffusion Coefficients (D), Diffusion Selectivities (D_i/D_j), Solubility Coefficients (S), and Solubility Selectivities (S_i/S_j) for Representative Hydroxyl-Containing Polyimide and Thermally Rearranged Polymer Membranes at 25 °C

			D (10^{-8} cm^2 s^{-1})				D_i/D_j			S (cm^3 [STP] cm^{-3} bar^{-1})				S_i/S_j		
polymer	batch	history	O_2	N_2	CO_2	CH_4	O_2/N_2	CO_2/N_2	CO_2/CH_4	O_2	N_2	CO_2	CH_4	O_2/N_2	CO_2/N_2	CO_2/CH_4
T-PIM-PI-OH-1	HS148	as cast	7.61	1.90	2.44	0.32	4.01	1.28	7.63	1.64	1.22	24.9	5.40	1.34	20.41	4.61
T-PIM-PBO-1	HS148	as prepared	27.7	7.80	12.2	1.84	3.55	1.56	6.63	1.89	1.57	21.4	6.33	1.20	13.63	3.38
		ethanol-treated	62.4	19.7	28.5	5.53	3.17	1.45	5.15	2.25	1.97	24.9	7.62	1.14	12.64	3.27
O-PIM-PI-OH-1	HS84	as cast	1.7	0.48	0.55	0.08	3.54	1.15	6.88	1.9	1.31	32.8	6.2	1.45	25.04	5.29
O-PIM-PBO-1	HS84	as prepared	13.7	3.75	5.83	0.86	3.65	1.55	6.78	2.60	2.13	33.0	9.07	1.22	15.49	3.64
		ethanol-treated	61.1	20.0	25.0	4.7	3.06	1.25	5.32	2.77	2.41	35.3	10.4	1.15	14.65	3.39
		aged 270 days	24.8	7.43	9.96	1.57	3.34	1.34	6.34	3.35	2.61	42.5	12.3	1.28	16.28	3.46
Copol-PBO-(1−2)	HS161	as prepared	24.2	6.56	9.38	1.38	3.69	1.43	6.80	1.83	1.53	24.0	5.60	1.20	15.69	4.29
		ethanol-treated	63.7	19.5	27.3	5.08	3.27	1.40	5.37	2.56	2.21	31.3	9.09	1.16	14.16	3.44
PIM-PBO-3	HS130	as prepared	13.1	3.68	5.25	0.84	3.56	1.43	6.25	2.41	1.69	35.4	8.34	1.43	20.95	4.24
		ethanol-treated	30.7	8.33	11.4	2.21	3.69	1.37	5.16	3.28	3.16	57.2	13.5	1.04	18.10	4.24
		aged 197 days	11	2	3	1	5.50	1.50	3.00	2.61	2.49	50.7	9.70	1.05	20.36	5.23

In general, the thermal treatment enhances the gas permeability in the order He < H_2 < O_2 ≤ CO_2 < N_2 < CH_4, thus affecting more the transport of the less permeable species, in line with the typical trade-off behavior for permeability and selectivity.

The PBO membranes were treated with ethanol, which swells the membranes significantly. For instance, samples of O-PIM-PBO-1 batch HS84 and T-PIM-PBO-1 batch HS77 membranes showed increases of more than 10%, in both length and width. On drying, the original dimensions were almost entirely recovered. The lengths of samples were slightly (less than 2%) higher than the "as cast" state, indicating the formation of some excess free volume after ethanol treatment. For all the PBO membranes studied here, ethanol treatment led to significant increases in gas permeabilities, particularly for O-PIM-PBO-1 and Copol-PBO-(1−2) (Table 3). The permeability enhancement is coupled with corresponding decreases in selectivity. This is the typical behavior observed for PIMs and PIM-PIs.[13,23]

The two PIM-PI-OH-1 polyimides present the typical "size-selective" behavior of glassy polymers, with the smaller molecules (e.g., H_2 and He) being more permeable than the other species. O-PIM-PBO-1 shows a "reverse selectivity" after thermal rearrangement and thus allows a faster transport of CO_2 with respect to H_2 and He. It maintains this feature also upon ethanol soaking. The other PIM-PBO membranes present an intermediate behavior with the following permeation order in the "as prepared" samples: H_2 > CO_2 > He. The ethanol treatment of these PBO membranes results again in a higher permeability for CO_2 with respect to the other gases and thus in a partial loss of the molecular sieving character and increased solubility−selectivity. In any case, the ethanol treatment produces also an inversion of the permeability for CH_4 and N_2, with a slightly higher permeability for the hydrocarbon molecule.

Over time, permeabilities then reduce and selectivities increase, as can be seen in Table 3 for O-PIM-PBO-1 and PIM-PBO-3. In particular, the aged PIM-PBO-3 becomes even more size selective than the "as prepared" state. For O-PIM-PBO-1, nine months after ethanol treatment, permeabilities are still higher than for the "as cast" membrane, suggesting that removal of residual solvent is a significant factor. In contrast, in the case of PIM-BO-3, six and a half months after ethanol treatment, permeabilities have returned to values similar to the "as prepared" membrane, suggesting that the primary effect of ethanol treatment is the introduction of excess free volume that is readily lost by physical aging.

The trade-off between selectivity and permeability for polymeric membranes is frequently represented on double-logarithmic "Robeson" plots.[14,15] In Figure 5, data for "as prepared" and "ethanol-treated" PBO membranes from this work are reported for three technologically relevant separations: CO_2/N_2, CO_2/CH_4, and O_2/N_2. These data are also compared with those reported by Li et al.[52] for membranes obtained by thermal treatment of other spiro-containing hydroxyl-functionalized polyimides. It is noteworthy that for the CO_2/N_2 pair PIM-PBO-3 shows improved selectivity compared to other spiro-containing TR polymers subjected to similar thermal treatments. It has been shown by Ma et al.[53] that even higher selectivities can be achieved by treatments at higher temperature (from 530 to 800 °C), effectively leading to an amorphous carbon and then to its graphitic molecular sieve membrane by carbonization.

dx.doi.org/10.1021/ma5011183 | Macromolecules 2014, 47, 5595−5606

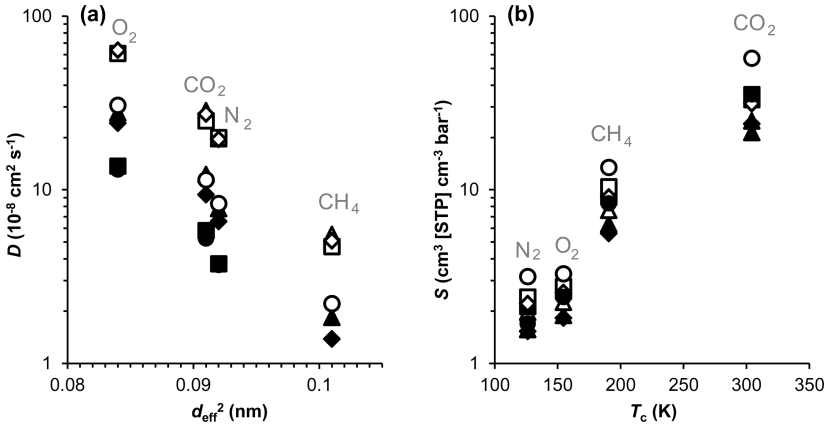

Figure 6. Plots of (a) gas diffusion coefficient versus the square of the effective diameter of the gas, d_{eff}^2, and (b) solubility coefficient versus critical temperature of the gas, T_c, for as prepared (solid symbols) and ethanol-treated (open symbols) membranes of T-PIM-PBO-1 batch HS148 (▲, △), O-PIM-PBO-1 batch HS84 (■, □), Copol-PBO-(1−2) (◆, ◇), and PIM-PBO-3 (●, ○).

Diffusion coefficients D, determined from the time lag, and apparent solubility coefficients S, calculated from the relationship $P = D \times S$, are listed in Table 4 for four gases with a sufficiently long time lag for D to be determined with >90% accuracy. Ideal diffusion and solubility selectivities for the gas pairs O_2/N_2, CO_2/N_2, and CO_2/CH_4 are also included in Table 4. Diffusion selectivity dominates for O_2/N_2, and solubility selectivity for CO_2/N_2, whereas both diffusion and solubility contribute significantly to the overall selectivity for CO_2/CH_4. The data in Table 4 show that the enhanced permeability after thermal rearrangement and after ethanol treatment is almost entirely due to faster diffusion, increasing by an order of magnitude or more for all gas species. The solubility, on the other hand, changes much less, generally not more than a factor of 1.5−2. This demonstrates the strong correlation between the diffusion coefficient and the free volume or microporosity of the polymers. Various correlations between the transport parameters of gases in the polymer matrix and the molecular properties of the gas have been proposed.[60] The diffusion coefficient typically scales with the square of the molecular diameter. For "as prepared" and "ethanol-treated" PBO membranes, values of D are plotted in Figure 6a against the squared effective diameter of the gas,[61] and values of S are plotted in Figure 6b against the critical temperature of the gas. The plots confirm that D decreases with increasing gas diameter and S increases with increasing critical temperature of the penetrant, as was also reported for other PIM-PIs and for PIM-1.[23] Strong interactions with the polymer, whether through enhanced adsorption in narrow micropores, or through specific interactions with functional groups, may have the effect of depressing CO_2 diffusion,[62] as has recently been demonstrated for amine-modified PIM-1,[63] but that effect is not observed here.

■ CONCLUSIONS

Two spiro-center-containing dianhydrides were successfully utilized in the preparation of hydroxyl-functionalized polyimides with significant internal surface area and with interconnected free volume. Dianhydride An-1 gave more robust membranes than An-2, which lacks the relatively flexible dibenzodioxin linkage. The PIM-PI-OH materials were thermally treated at 450 °C, yielding thermally rearranged polymers with enhanced performance for gas separation membranes and increased solvent resistance. The transport properties of the thermally rearranged polymers can be tailored through the choice of the diamine used to prepare the precursor. The highly compact diamine 4,6-diaminoresorcinol (DAR) gives PIM-PBO-3 membranes which are equally permeable but more selective for CO_2/N_2 than the PIM-PBO-1 samples based on the (2,2-bis(3-amino-4-hydroxyphenyl)hexafluoropropane (bisAPAF) diamine. For all polymers the TR reaction and the ethanol treatment of the membranes enhance drastically the diffusion coefficient, while the solubility increases only modestly, confirming the important role of the free volume and microporosity on the gas diffusion. Together with parallel work demonstrating that more intense thermal treatments may enhance molecular sieve behavior,[53] this research opens up further opportunities for membrane development.

■ AUTHOR INFORMATION

Corresponding Author

*E-mail Peter.Budd@manchester.ac.uk; Tel +44(0)161-275-4711 (P.M.B.).

Notes

The authors declare no competing financial interest.

■ ACKNOWLEDGMENTS

The work leading to these results has received funding from the UK Engineering and Physical Sciences Research Council (EPSRC Grant EP/G062129/1, Innovative Gas Separations for Carbon Capture), from the European Community's Seventh Framework Programme (FP7/2007-2013) under grant agreement no. NMP3-SL-2009-228631 (project Double-NanoMem), and from the Italian national research program "Programma Operativo Nazionale Ricerca e Competitività 2007-2013, project PON01_01840 MicroPERLA". We are grateful to Mr. Gareth Smith for analysis by MALDI mass spectrometry and to Mr. Fabio Bazzarelli for assistance in some of the gas permeation tests.

■ ABBREVIATIONS

An-1, An-2, dianhydrides with structures shown in Figure 1; ATR, attenuated total reflectance; BET, Brunauer−Emmet−Teller; bisAPAF, 2,2-bis(3-amino-4-hydroxyphenyl)-hexafluoropropane; DAR, 4,6-diaminoresorcinol; DMAc, dimethylacetamide; DMN, 3,3′-dimethylnaphthidine; 6FDA, 4,4′-

(hexafluoroisopropylidene)diphthalic anhydride; IR, infrared; IUPAC, International Union of Pure and Applied Chemistry; MALDI-TOF MS, matrix assisted laser desorption/ionization−time-of-flight mass spectrometry; NMP, *N*-methyl-2-pyrrolidone; NMR, nuclear magnetic resonance; O, one-pot polycondensation method of polyimide formation; PAA, poly(amic acid); PBO, polybenzoxazole; PI, polyimide; PIM, polymer of intrinsic microporosity; T, thermal imidization method of polyimide formation; THF, tetrahydrofuran; TMDA, 2,3,5,6-tetramethyl-1,4-phenylenediamine; TSDD, 3,3,3′,3′-tetramethyl-1,1′-spirobisindane-5,5′-diamino-6,6′-diol.

REFERENCES

(1) Bernardo, P.; Drioli, E.; Golemme, G. *Ind. Eng. Chem. Res.* **2009**, *48*, 4638−4663.
(2) Sanders, D. F.; Smith, Z. P.; Guo, R.; Robeson, L. M.; McGrath, J. E.; Paul, D. R.; Freeman, B. D. *Polymer* **2013**, *54*, 4729−4761.
(3) Budd, P. M.; McKeown, N. B. *Polym. Chem.* **2010**, *1*, 63−68.
(4) Du, N.; Park, H. B.; Dal-Cin, M. M.; Guiver, M. D. *Energy Environ. Sci.* **2012**, *5*, 7306−7322.
(5) McKeown, N. B. *ISRN Materials Science* 2012, 513986, 513916 pp.
(6) McKeown, N. B.; Budd, P. M. *Macromolecules* **2010**, *43*, 5163−5176.
(7) McKeown, N. B.; Budd, P. M. *Chem. Soc. Rev.* **2006**, *35*, 675−683.
(8) Budd, P. M.; Ghanem, B. S.; Makhseed, S.; McKeown, N. B.; Msayib, K. J.; Tattershall, C. E. *Chem. Commun.* **2004**, 230−231.
(9) Everett, D. H. *Pure Appl. Chem.* **1972**, 577−638.
(10) Budd, P. M.; McKeown, N. B.; Fritsch, D. *J. Mater. Chem.* **2005**, *15*, 1977−1986.
(11) Budd, P. M.; Elabas, E. S.; Ghanem, B. S.; Makhseed, S.; McKeown, N. B.; Msayib, K. J.; Tattershall, C. E.; Wang, D. *Adv. Mater.* **2004**, *16*, 456−459.
(12) Budd, P. M.; Msayib, K. J.; Tattershall, C. E.; Ghanem, B. S.; Reynolds, K. J.; McKeown, N. B.; Fritsch, D. *J. Membr. Sci.* **2005**, *251*, 263−269.
(13) Budd, P. M.; McKeown, N. B.; Ghanem, B. S.; Msayib, K. J.; Fritsch, D.; Starannikova, L.; Belov, N.; Sanfirova, O.; Yampolskii, Y.; Shantarovich, V. *J. Membr. Sci.* **2008**, *325*, 851−860.
(14) Robeson, L. M. *J. Membr. Sci.* **1991**, *62*, 165−185.
(15) Robeson, L. M. *J. Membr. Sci.* **2008**, *320*, 390−400.
(16) Cecopieri-Gomez, M. L.; Palacios-Alquisira, J.; Dominguez, J. M. *J. Membr. Sci.* **2007**, *293*, 53−65.
(17) Xiao, Y.; Low, B. T.; Hosseini, S. S.; Chung, T. S.; Paul, D. R. *Prog. Polym. Sci.* **2009**, *34*, 561−580.
(18) Tanaka, K.; Okano, M.; Toshino, H.; Kita, H.; Okamoto, K. *J. Polym. Sci., Part B: Polym. Phys.* **1992**, *30*, 907−914.
(19) Nagel, C.; Guenther-Schade, K.; Fritsch, D.; Strunskus, T.; Faupel, F. *Macromolecules* **2002**, *35*, 2071−2077.
(20) Zhang, Q.; Chen, G.; Zhang, S. *Polymer* **2007**, *48*, 2250−2256.
(21) Ghanem, B. S.; McKeown, N. B.; Budd, P. M.; Selbie, J. D.; Fritsch, D. *Adv. Mater.* **2008**, *20*, 2766−2771.
(22) Ghanem, B. S.; McKeown, N. B.; Budd, P. M.; Al-Harbi, N. M.; Fritsch, D.; Heinrich, K.; Starannikova, L.; Tokarev, A.; Yampolskii, Y. *Macromolecules* **2009**, *42*, 7881−7888.
(23) Rogan, Y.; Starannikova, L.; Ryzhikh, V.; Yampolskii, Y.; Bernardo, P.; Bazzarelli, F.; Jansen, J. C.; McKeown, N. B. *Polym. Chem.* **2013**, *4*, 3813−3820.
(24) Park, H. B.; Jung, C. H.; Lee, Y. M.; Hill, A. J.; Pas, S. J.; Mudie, S. T.; Van Wagner, E.; Freeman, B. D.; Cookson, D. J. *Science* **2007**, *318*, 254−258.
(25) Park, H. B.; Han, S. H.; Jung, C. H.; Lee, Y. M.; Hill, A. J. *J. Membr. Sci.* **2010**, *359*, 11−24.
(26) Han, S. H.; Misdan, N.; Kim, S.; Doherty, C. M.; Hill, A. J.; Lee, Y. M. *Macromolecules* **2010**, *43*, 7657−7667.
(27) Calle, M.; Chan, Y.; Jo, H. J.; Lee, Y. M. *Polymer* **2012**, *53*, 2783−2791.
(28) Wang, H.; Liu, S.; Chung, T.-S.; Chen, H.; Jean, Y.-C.; Pramoda, K. P. *Polymer* **2011**, *52*, 5127−5138.
(29) Kim, S.; Lee, Y. M. *J. Nanopart. Res.* **2012**, *14*, 949/941−949/911.
(30) Kim, S.; Jo, H. J.; Lee, Y. M. *J. Membr. Sci.* **2013**, *441*, 1−8.
(31) Sanders, D. F.; Smith, Z. P.; Ribeiro, C. P., Jr.; Guo, R.; McGrath, J. E.; Paul, D. R.; Freeman, B. D. *J. Membr. Sci.* **2012**, *409−410*, 232−241.
(32) Guo, R.; Sanders, D. F.; Smith, Z. P.; Freeman, B. D.; Paul, D. R.; McGrath, J. E. *J. Mater. Chem. A* **2013**, *1*, 262−272.
(33) Guo, R.; Sanders, D. F.; Smith, Z. P.; Freeman, B. D.; Paul, D. R.; McGrath, J. E. *J. Mater. Chem. A* **2013**, *1*, 6063−6072.
(34) Choi, J. I.; Jung, C. H.; Han, S. H.; Park, H. B.; Lee, Y. M. *J. Membr. Sci.* **2010**, *349*, 358−368.
(35) Jung, C. H.; Lee, J. E.; Han, S. H.; Park, H. B.; Lee, Y. M. *J. Membr. Sci.* **2010**, *350*, 301−309.
(36) Soo, C. Y.; Jo, H. J.; Lee, Y. M.; Quay, J. R.; Murphy, M. K. *J. Membr. Sci.* **2013**, *444*, 365−377.
(37) Calle, M.; Lee, Y. M. *Macromolecules* **2011**, *44*, 1156−1165.
(38) Yeong, Y. F.; Wang, H.; Pallathadka Pramoda, K.; Chung, T.-S. *J. Membr. Sci.* **2012**, *397−398*, 51−65.
(39) Hodgkin, J. H.; Dao, B. N. *Eur. Polym. J.* **2009**, *45*, 3081−3092.
(40) Hodgkin, J. H.; Liu, M. S.; Dao, B. N.; Mardel, J.; Hill, A. J. *Eur. Polym. J.* **2011**, *47*, 394−400.
(41) Kostina, J.; Rusakova, O.; Bondarenko, G.; Alentiev, A.; Meleshko, T.; Kukarkina, N.; Yakimanskii, A.; Yampolskii, Y. *Ind. Eng. Chem. Res.* **2013**, *52*, 10476−10483.
(42) Calle, M.; Lozano, A. E.; Lee, Y. M. *Eur. Polym. J.* **2012**, *48*, 1313−1322.
(43) Jiang, Y.; Willmore, F. T.; Sanders, D.; Smith, Z. P.; Ribeiro, C. P.; Doherty, C. M.; Thornton, A.; Hill, A. J.; Freeman, B. D.; Sanchez, I. C. *Polymer* **2011**, *52*, 2244−2254.
(44) Park, C. H.; Tocci, E.; Lee, Y. M.; Drioli, E. *J. Phys. Chem. B* **2012**, *116*, 12864−12877.
(45) Smith, Z. P.; Sanders, D. F.; Ribeiro, C. P.; Guo, R.; Freeman, B. D.; Paul, D. R.; McGrath, J. E.; Swinnea, S. *J. Membr. Sci.* **2012**, *415−416*, 558−567.
(46) Smith, Z. P.; Tiwari, R. R.; Murphy, T. M.; Sanders, D. F.; Gleason, K. L.; Paul, D. R.; Freeman, B. D. *Polymer* **2013**, *54*, 3026−3037.
(47) Belov, N. A.; Nizhegorodova, Y. A.; Kim, S.; Han, S. H.; Yampolskii, Y. P.; Lee, Y. M. *Ind. Eng. Chem. Res.* **2013**, *52*, 10467−10475.
(48) Comer, A. C.; Ribeiro, C. P.; Freeman, B. D.; Kalakkunnath, S.; Kalika, D. S. *Polymer* **2013**, *54*, 891−900.
(49) Kim, S.; Han, S. H.; Lee, Y. M. *J. Membr. Sci.* **2012**, *403−404*, 169−178.
(50) Han, S. H.; Doherty, C. M.; Marmiroli, B.; Jo, H. J.; Buso, D.; Patelli, A.; Schiavuta, P.; Innocenzi, P.; Lee, Y. M.; Thornton, A. W.; Hill, A. J.; Falcaro, P. *Small* **2013**, *9*, 2277−2282.
(51) Ma, X.; Swaidan, R.; Belmabkhout, Y.; Zhu, Y.; Litwiller, E.; Jouiad, M.; Pinnau, I.; Han, Y. *Macromolecules* **2012**, *45*, 3841−3849.
(52) Li, S.; Jo, H. J.; Han, S. H.; Park, C. H.; Kim, S.; Budd, P. M.; Lee, Y. M. *J. Membr. Sci.* **2013**, *434*, 137−147.
(53) Ma, X.; Swaidan, R.; Teng, B.; Tan, H.; Salinas, O.; Litwiller, E.; Han, Y.; Pinnau, I. *Carbon* **2013**, *62*, 88−96.
(54) Swaidan, R.; Ma, X.; Litwiller, E.; Pinnau, I. *J. Membr. Sci.* **2013**, *447*, 387−394.
(55) Moy, T. M.; McGrath, J. E. *J. Polym. Sci., Part A: Polym. Chem.* **1994**, *32*, 1903−1908.
(56) Mason, C. R.; Maynard-Atem, L.; Al-Harbi, N. M.; Budd, P. M.; Bernardo, P.; Bazzarelli, F.; Clarizia, G.; Jansen, J. C. *Macromolecules* **2011**, *44*, 6471−6479.
(57) Crank, J. *The Mathematics of Diffusion*, 2nd ed.; Clarendon Press: Oxford, 1975.
(58) Wijmans, J. G.; Baker, R. W. *J. Membr. Sci.* **1995**, *107*, 1−21.
(59) Carta, M.; Malpass-Evans, R.; Croad, M.; Rogan, Y.; Jansen, J. C.; Bernardo, P.; Bazzarelli, F.; McKeown, N. B. *Science* **2013**, *339*, 303−307.

(60) *Materials Science of Membranes for Gas and Vapor Separation*; Yampolskii, Y., Pinnau, I., Freeman, B. D., Eds.; Wiley: Chichester, 2006.
(61) Teplyakov, V.; Meares, P. *Gas Sep. Purif.* **1990**, *4*, 66−74.
(62) Lin, H.; Freeman, B. D. *J. Mol. Struct.* **2005**, *739*, 57−74.
(63) Mason, C. R.; Maynard-Atem, L.; Heard, K. W. J.; Satilmis, B.; Budd, P. M.; Friess, K.; Lanc, M.; Bernardo, P.; Clarizia, G.; Jansen, J. C. *Macromolecules* **2014**, *47*, 1021−1029.